Quantitative Mineralogy to Assess Waste Rock Weathering at the Antamina Mine

[*]Randy Blaskovich[1], Bern Klein[2], Stephane Brienne[1], Roger D. Beckie[3], K. Ulrich Mayer[3], Celedonio A. Aranda[4], Charlene Haupt[2]

[1] Teck Metals Ltd., Trail, BC, V1R 4S4, Canada
[2] Norman B. Keevil Institute of Mining Engineering, University of British Columbia, Vancouver, BC, V6T 1Z4, Canada
[3] Dept. of Earth and Ocean Sciences, University of British Columbia, Vancouver, BC, V6T 1Z4, Canada
[4] Compañia Minera Antamina S.A., Lima 41, Perú
([*]Corresponding author: randy.blaskovich@teck.com)

Key words: Mineral Liberation Analyzer, classification, liberation analysis, association, mineral processing, modeling

Abstract
Quantitative mineralogy was developed for use in mineral processing by combining scanning electron microscopy, energy dispersive X-ray analysis and image analysis. Many of the same mineralogical features important in mineral recovery are important to weathering and metal leaching processes in mine wastes. The Mineral Liberation Analyzer (MLA) can be used to facilitate assessment of potential long-term weathering behaviour in natural processes such as acid rock drainage (ARD). This paper describes mineralogical factors relevant to mineral weathering and demonstrates the application of the MLA to provide quantitative information.

A quantitative mineralogical study was conducted on waste rock from the Antamina Mine operation in Peru. The MLA results can quantify the availability of reactive minerals, reaction of alkaline-consuming minerals and reactions that result in the formation of secondary mineral phases. In Antamina Mine waste rock, the MLA was used to identify primary and secondary phases that sequester weathering products, including mineral associations, mineral liberation and grain size. The results from the MLA can be used to develop and improve waste rock classification systems. Better classification of the reactivity of the rock will lower projected costs for mine closure and improve environmental waste management.

Introduction
The focus of this study was to develop and assess the use of MLA technology to locate and quantify an element of concern (EOC) in a natural waste rock environment with the intent of providing useful information to improve weather modeling. The MLA is a quick method to determine EOC trace levels (and associated mineralogy) and mineral of interest (MOI) distributions. This paper will use some of these EOCs to feature output resulting from the MLA analysis. This technology approach could also be applied to tailings disposal and heap leach activity. This work will demonstrate the usefulness of the MLA to aid understanding of weathering mechanisms through highlighting MLA software features.

The minerals in any deposit are associated with each other according to natural rock-forming processes. There are three basic types of ore deposits: (1) sulphide; (2) non-sulphide, which fall into two types, hypogene (usually oxidized) or supergene (absence of sulphide mineralogy and at/near surface exposure) weathering; and, (3) mixed sulphide-oxide. In many parts of the world the highest grade mineral deposits are being depleted and are not replaced by new high-grade deposits. The first type of deposit is no longer the “norm” and the significant deposits of today are usually complex mixed sulphide-oxide ores. Because of their complex nature, these ores are a challenge in mineral processing and often, parts of the deposit will not be processed for metallurgical and/or economic reasons. This material is placed in waste rock dumps.

Description of ore texture is a complex topic. In petrography, ore texture describes the micro- or meso-scale features that characterize a particular lithology and is defined by the size, shape, arrangement, orientation and distribution of the mineral components. Additionally, the definition might include a particle description, ranging from mineral grains on a micron scale up to pieces of rock on a centimetre scale.

Geologists classify texture based upon the origin of the rock in which the texture formed and the minerals enclosed [Atkinson and Erickson 1984]. Mining engineers and metallurgists generally design processes to optimize the recovery rate and grade of valuable minerals while minimizing handling costs, with little attention to the texture and mineralogy which can affect the recovery and grade [Petruk 2000]. Geochemists, similar to engineers, focus on concentrations of metals though may extrapolate to mineralogy and leaching mechanisms. The importance of texture and mineralogy cannot be ignored as it affects the way metals and EOCs are extracted. The environmental engineer considers whole rock composition (both elementally and mineralogically) to determine the best rock drainage mitigation strategy. It should be noted that there is generally no financial benefit in processing mine wastes even though, quite often, there are associated environmental and financial liabilities.

Characterization of waste rock leaching requires a thorough understanding of naturally occurring chemical processes. To model successfully it is necessary to understand mineral phase interactions (eg chemical and galvanic) and weathering/leaching mechanisms (eg chemistry and flow processes, oxygen uptake, diffusion through inter-particle pores, microbe activity, particle mineral phase distribution and availability to weathering, surface chemical and electrochemical interactions). Research on the characterization of waste rock using automated mineralogical instrumentation (eg MLA technology) is limited. The MLA is capable of analyzing waste rock in terms of such mineralogical factors as modal mineralogy, particle/grain-size distribution, mineral association and EOC availability (ie encapsulated or degree of exposure).

Background

Waste rock is formed by blasting non-ore grade material during mining operations. It typically contains a wide range of particle sizes (eg 1-metre boulders to sub-micrometer grains) resulting in a very complex granular mass. The large-scale internal structure of a waste rock pile will vary from random orientation to compacted layers. Storage of mine waste can generate EOC-containing acidic waters and secondary minerals. Secondary minerals may also dissolve, further complicating modeling of the acid-rock or neutral-rock drainage (NRD). The balance between the rates of acid production by minerals such as iron-sulphide oxidation and host-rock mineral neutralization will determine the acidity of waste rock drainage. One of the most effective minerals for neutralizing acid is carbonate, such as calcite ($CaCO_3$). The defining line between ARD and NRD is approximately pH 6.4 [Drever, 1988; Alpers *et al*. 1994] as shown by equation 1 which represents the dominant acid-neutralizing reaction of calcite above pH 6.4, and equation 2 showing the dominant reaction below pH 6.4:

$$CaCO_{3(s)} + H^+_{(aq)} = HCO_3^-{}_{(aq)} + Ca^{2+}_{(aq)} \quad (1)$$

$$CaCO_{3(s)} + 2H^+_{(aq)} = H_2CO_{3(aq)} + Ca^{2+}_{(aq)} \quad (2)$$

It is necessary to identify the secondary mineral phases to better determine how dissolution, oxidation and precipitation of mineral phases occur in waste rock weathering reactions. This can be accomplished through detailed mineralogical study of the liberation/exposure and associations of the reactants and products. The texture of the rock provides access to the minerals, through fine and coarse-grained particles, mineral boundaries, solid solution chemistry and availability of EOC.

In mineral processing, the liberation size is a measure of the inherent textural relationships between ore minerals. The process of liberation is the size to which an ore must be crushed or ground to separate economic minerals and waste with an acceptable efficiency by a commercial process. The concept of liberation size and process of liberation may be extended to ARD or NRD prediction, where atmospheric leaching becomes the relevant process. For example, atmospheric pyrite oxidation requires at least a part of the mineral grain to be exposed for leaching. For any given pyritic rock, the degree of pyrite mineral grain exposure increases with decreasing particle size, attaining 100% exposure or liberation for leaching when all of the rock has been reduced in size to that of the smallest grain of pure pyrite. For rock drainage prediction the important characteristics of ore or waste are: (1) amount and types of sulphide minerals; (2)

the types and amounts of minerals containing EOCs; (3) the extent of liberation of sulphide and EOC minerals; (4) the association of sulphide minerals with other sulphide and non-sulphide minerals (eg carbonates, silicates).

Most ARD-related mineralogical studies have focused on the products of pyrite oxidation and the products of ARD neutralization within tailings and waste rock impoundments [Druschel *et al.* 2004; Wang *et al.* 2007]. It is easier to determine particle size distribution and liberation characteristics for tailings than it is for waste rock dumps (ie crush size is already defined). For existing tailings, size distribution may be representatively determined from screening results, while liberation characteristics are usually approximated by optical microscopy. It is usually possible to determine the frequency of occurrence of individual minerals within a sample by the examination of a number of microscopic fields of view. Quantitative mineralogical analysis by this method is termed modal analysis.

For existing waste rock dumps the acquisition of representative size distributions for testing is difficult since particle size ranges from the coarsest material produced by blasting to the finest material retained after rain and snow infiltration and flushing. Liberation characteristics for waste rock material may be (and usually are) inferred from examination of the finer dump material. Where only drill core is available, liberation characteristics might be determined by microscopy techniques, although estimated size distributions require information on the proposed mining method and milling flowsheet.

The static procedures used in the Antamina Mine waste rock test work all require that a sample be ground, so that liberation characteristics of acid-generating minerals and neutralizing minerals can be observed. In a waste rock pile a size fraction of -2 mm would be expected to have a relatively high degree of liberation of both acid-generating and neutralizing minerals when compared to the coarser fractions. The finer particles would display higher in-situ acid generation and neutralization with concurrent reduction in neutralizing potential and sulphide content. Other causes of differences between size fractions may be related to crystal structure; for example, after size reduction by impact, the friability of pyrite phases relative to calcite could lead to an increased quantity of liberated pyrite particles of a given size compared to calcite particles of the same size.

Challenges imposed when collecting samples include attention to fine grain size, water soluble mineral phases and precipitation reactions when in uncontrolled sample storage environments. The use of mineral chemistry in the classification of minerals is widely used; however, application to the mineral processing industry is still gaining acceptance [Chandra and Gerson 2009].

In the past, the tools available for the identification of phases controlling mine and rock drainage and for modeling ARD and NRD included optical microscopy, X-ray diffractometry (XRD), scanning electron microscopy (SEM) and chemical analysis [example: Álvarez-Valero *et al.* 2008]. A significant advancement occurred in the 1980s with the development of automated quantitative instrumentation to measure mineralogy and liberation characteristics, such as the MLA and the Quantitative Evaluation of Minerals by Scanning Electron Microscopy (QEMScan) [Gu 2003; Gotlieb *et al.* 2000]. This approach directly linked mineralogy and mineral processing data. Mineralogists are now able to augment information from the MLA using other techniques, including: optical, near-infrared, X-ray beam, laser beam, electron beam (SEM, electron probe micro-analysis (EPMA)), and proton beam techniques.

Today, process mineralogy is beginning to realize the value of the MLA and QEMScan techniques. A process mineralogy program might encompass such items as geology, sampling, hardness, mineralogy, and mineral processing [Lotter *et al.* 2003; McKay *et al.* 2007]. By integrating into a weathering model the EOC MOI particle size, shape and availability (or exposure) predictions can be improved. In this new approach to characterize waste rock, the automated quantitative MLA system can be used.

Experimental

The waste rock examined in this study was supplied by the Antamina Mine. The Antamina Mine (latitude 9° 32' S, longitude 77° 03' W) is in the Peruvian Andes range, 270 km north of Lima and 200 km west of Huarez, at approximately 4300 m above sea level. The Antamina Mine deposit is a large copper skarn with associated zinc, silver, lead, molybdenum and bismuth. It is hosted in high-neutralization capacity rock. Since mine start-up in 2001, about 300,000 tonnes of waste rock have been produced daily. There are five distinct waste rock types: hornfels, marble, skarn, intrusives, and limestone, with the vast majority being hornfels and marble. Currently, the Antamina Mine waste rock is categorized into three reactivity types for management purposes, Class A (reactive), Class B (moderately reactive) and Class C (less reactive) based upon metal content and visible staining [Table 1].

Table 1. Antamina Mine waste rock classification criteria[1], January 2010

Class	Reactivity	Rock Type	Zn (%)	As (%)	Visual Sulphide[1] (%)	Visual oxidation[2] (%)	Location
A	Reactive	Mineralized/ oxidized rock (including Skarn (endo/exo), Hornfels, Marble, Limestone (some Intrusives); high Zn, As, S	>0.15	>0.04	>3	>10	within pit limits; East dump
B	Moderately reactive	Hornfels, Marble and Limestone; moderate Zn	0.07-0.15	<0.04	2-3	<10	stockpile pads; construction material; Tucush or East dump
C	Less reactive	Hornfels, Marble and Limestone; low Zn, As, S	<0.07	<0.04	<2	Minimal / trace	wherever needed (e.g. East dump, Tucush dump, tailings dam, water reservoir dam, access roads)

[1] Antamina 2007, Ore Control Procedure Manual.

[2] visual oxidation criteria (e.g. Fe staining) only in effect during tailings dam construction.

The mineralogical samples examined at the microtexture scale were polished grain mounts. Typically, sub-1 mm broken rock is mounted in epoxy resin, and polished for examination by either optical microscope or SEM. The advantage of the polished grain mount is that a single mount can give good sampling statistics for a large composite of rock. For this introduction to MLA capabilities a "fresh" (ie unweathered) sample from the Tucush (01) waste rock dump will be highlighted. The Tucush waste rock dump contains Class B and C material.

A representative portion of the sample was subjected to a diagnostic leach procedure which was to mimic accelerated weathering. The basic diagnostic leach was developed in the 1980s to improve understanding of mineralogical interactions [see details: Lorenzen 1995]. Details of the method used in this study will be reported in a future publication. The sample was provided crushed and sized, with particles less than 1.9 mm provided for analysis. Each size fraction (see Table 2 for sizes) was air-dried, then riffled to a representative smaller sub-sample. Epoxy-mounted transverse grain mounts were prepared from the size fractions. The sample particles were mounted in transverse mounts to eliminate reporting errors in data collection due to particle density segregation. These mounts were prepared by mixing the sample with

resin, allowing the resin to cure in a cylinder, cutting the cylinder longitudinally, and polishing the cut surface.

The MLA comprises FEI Company's Quanta SEM equipped with a tungsten filament, dual Bruker-AXS silicon drift detectors and energy dispersive spectrometers (EDS) coupled with FEI's MLA software. The MLA analyzed the grain mounts to spectral resolution 150eV (full-width half-maximum) for X-ray analysis and 0.1 µm for spatial analysis to provide mineralogical and textural information. The elemental detection limits range from 0.1-0.5 wt% depending upon the quality of the sample mount surface being analyzed.

Once the polished mounted sample is in the evacuated SEM vacuum chamber, data acquisition parameters need to be applied. These include: accelerating voltage, spot size and frame resolution, dwell time and acquisition time, back-scatter electron (BSE) gray level strategy, beam optimization, and mineral classification criteria. The MLA provides a range of pre-programmed analysis modes: XMOD – modal mineralogy, no particle detail; XBSE – modal mineralogy, particle detail; (G)XMAP – modal mineralogy, improved particle detail; and, SPL (XBSE, XMAP, DZ, X) – specific to MOI or EOC via BSE gray level. In this study, the XBSE mode of analysis was used after consideration of analysis time and particle detail required. The automated imaging and X-ray analysis technology integrates with automated stage control to enable measurement of a prescribed number of grains or particles (eg 4000 particles for mine concentrate; greater than 50,000 particles for mine tailing).

While the mounted sample is being analyzed on-line, a BSE gray level image is recorded along with a segmented false-colour image (which delineates the mineral phases in each particle). Each segmented phase in the particle is compared to the X-ray classification standard (created from directly observed mineralogy in the sample mass provided) to identify the mineral phase. Off-line, the operator then checks the image data for focus, BSE stability, MLA reconciliation to chemical assay data (from ICP and AAS analysis) and finally processes data into a database which contains all sample particles analyzed and their associated numerical data (eg bulk mineralogy; particle size distribution; liberation, association and surface exposure of MOIs; shape characteristics). For more details on MLA operation see Gu [2003] and Fandrich *et al.* [2007].

Results and Discussion

This study of Antamina Mine waste rock represents a valuable opportunity to characterize mineralogy and determine geochemical mechanisms for weathering products. A significant achievement was the development of an extensive MLA X-ray mineral classification database. The mineral database was created using an MLA mode of analysis to locate the unknown mineral phases rapidly, after which they were carefully examined using EDS and assigned a mineral name. The database contains minerals located by the MLA, keeping in mind that the majority of secondary mineral phases are usually represented by little surface area which will challenge SEM resolution. A slow and methodical examination of every particle, using a higher resolution microscope equipped with EPMA, would improve the database.

Table 2 displays the modal mineralogy for each size fraction analysed based on particle count, before and after exposure to a diagnostic sequential leach (see Appendix for complete list of EOC-specific mineral phases). Table 2 data shows that the diagnostic leach significantly reduced carbonate presence and increased sulphide exposure, suggesting (and verified by reviewing particles) the leach led to increased exposure of sulphide grain inclusions to acid generation. After leaching, the sub-297 µm MOI iron hydroxide (denoted as FeOxyhydroxides) particles had a decreased presence while iron sulphate (denoted as FeSulphate) had an increased presence. Both phases had sequestered trace arsenic within their EDS determined composition. This may indicate that arsenic associated with sulphate phases is resistant to weathering. Further investigation of the reactivity of sub-297 µm waste rock particles and/or iron sulphate armouring could be pursued in another study.

The diagnostic leach, an accelerated example of weathering, did cause exposure and consequent leaching of sulphide particles. The leach, in conjunction with MLA analysis, will lead to improved waste rock type classification and waste rock management. SEM detection limits would prevent credible detection of the presence of the trace arsenic incorporated in phases; however, because the phase had been located by MLA and a composition included in the classification database, arsenic could be reported (note: many occurrences were verified visually by driving the SEM stage to the sample particle position and using EDS analysis).

Table 2. MLA overall modal mineralogy: before and after diagnostic sequential leach

Mineral group	Sample	Before Leach (# particles)					After Leach (# particles)			
	Mineral \ µm	-1190/+600	-600/+297	-297/+105	-105/+53	-53	-1190/+600	-297/+105	-105/+53	-53
Sulphide	Bornite	1	2	1	6	0	0	1	1	0
	Galena	20	58	28	56	12	10	919	242	564
	Sphalerite	36	97	68	136	50	49	54	248	267
	Chalcopyrite	34	116	195	200	77	121	365	245	453
	Pyrrhotite	348	492	238	410	138	654	1743	2553	2239
	Realgar-Orpiment	0	0	0	0	0	0	0	0	0
	Stibnite	0	4	1	8	1	2	3	1	64
	Watanabeite	1	2	1	5	1	0	107	272	923
	Pyrite	649	1095	404	968	348	1343	3603	4429	4722
	Molybdenite	3	16	98	22	2	3	2424	2131	356
	Enargite	0	2	1	5	1	2	120	194	353
	Other	5	22	36	30	1	6	2662	8116	6967
Subtotal		**1097**	**1906**	**1071**	**1846**	**631**	**2190**	**12001**	**18432**	**16908**
Carbonate	Calcite	23454	46389	51101	82431	48377	13115	11673	3597	1449
	Otavite	0	0	0	0	0	0	0	0	0
	Siderite	29	51	27	114	36	9	4	10	1
	Dolomite	32	73	1041	81	25	67	79	15	0
	Other	61	193	185	321	145	164	93	37	35
Subtotal		**23576**	**46706**	**52354**	**82947**	**48583**	**13355**	**11849**	**3659**	**1485**
Silicate	Biotite	1906	3284	3433	4490	3454	10265	79416	94385	165083
	Chlorite	603	551	570	438	209	913	3407	5281	8091
	K_Feldspar	802	1118	954	1603	805	2142	4083	5933	4250
	Kaolinite	13	37	272	41	12	32	2563	1136	2154
	Muscovite	38	36	1166	79	12	31	880	1781	1585
	Plagioclase	7982	22271	23609	27520	14470	37600	67100	71403	82076
	Pyroxene	1443	2792	3011	3489	1264	4321	8657	8398	3714
	Quartz	4997	5823	7941	7012	4011	13474	20020	22834	33017
	Talc	0	7	1	4	1	2	0	0	0
	Mica	1298	1395	1879	2383	1365	3094	11995	17386	12726
	Titanite	498	966	615	937	326	1398	4605	6489	9263
	Wollastonite	749	1497	1594	1583	293	1947	86	102	10
	Other	1618	3159	2792	3449	1172	7183	4149	2538	1061
Subtotal		**21947**	**42936**	**47837**	**53028**	**27394**	**82402**	**206961**	**237666**	**323030**
Phosphate		410	806	546	723	173	886	2279	614	509
Oxide	FeOxyhydroxides	204	403	930	436	121	281	407	608	725
	Other	22	52	145	65	30	13	1820	1447	459
Subtotal		**226**	**455**	**1075**	**501**	**151**	**294**	**2227**	**2055**	**1184**
Sulphate	FeSulphate	245	482	522	694	264	313	1876	2514	4056
	Barite	4	7	15	7	3	5	1074	78	0
	Gypsum	162	616	776	362	56	48	5	11	1
	Other	2	9	13	8	0	1	1	2	9
Subtotal		**413**	**1114**	**1326**	**1071**	**323**	**367**	**2956**	**2605**	**4066**
Other		59	195	237	226	63	87	6151	1541	1898
Total		**47728**	**94118**	**104446**	**140342**	**76332**	**208643**	**244425**	**267115**	**349081**

Under oxidizing conditions, the EOC secondary minerals may have high mobility but could also provide solubility control (eg iron sulphate). Arsenic-specific MOI information available through the MLA database is seen in Table 3. Secondary mineral phases are often tiny, challenging the resolution of the SEM, and hence not all unique phases could be isolated and identified; nonetheless, the speed of the analysis does deliver fast useful information. Most of the arsenic associated with the phases is either part of the mineral lattice, interstitially in the lattice, as a grain inclusion or absorbed/adsorbed to a particle surface. As a consequence of the acid leach, the arsenic-bearing phases became exposed and likely sequestered in the newly formed sulphates as evidenced by an increase in the number of these particles. Interestingly, the number of arsenic-bearing iron oxyhydroxides changed little in the smallest particle size, indicating a phase and size that has little mobility and higher resistance to the weathering environment.

Table 3. MLA EOC arsenic distribution by mineral species: before and after diagnostic sequential leach

Sample	Before Leach (#particles)					After Leach (#particles)			
Mineral — µm	-1190/+600	-600/+297	-297/+105	-105/+53	-53	-1190/+600	-297/+105	-105/+53	-53
Arsenopyrite	0	0	no data	0	0	0	0	0	0
Enargite	0	0		0	0	0	2	0	0
FeOxyhydroxides	178	329		368	108	155	307	499	102
FeSulphate	234	442		612	230	577	2479	4525	885
Fornacite	0	0		0	0	0	0	0	0
Molybdofornacite	4	31		31	2	13	87	89	6
RealgarOrpiment	0	0		0	0	0	0	0	0
Siderite	29	51		114	36	9	29	23	2
Tennantite	0	1		1	0	3	5	19	2
Tyrolite	0	0		0	0	0	0	0	0
Watanabeite	1	2		5	1	4	12	17	4
No Arsenic Presence	42666	84738		129939	76009	319513	361864	629079	109518

Figure 1 shows an example of a false-coloured MLA particle map from a transverse polished grain mount. The one-hour MLA XBSE analysis analyzed a minimum of 20,000 particles from each size fraction. During the epoxy curing process the particles segregate due to density differences, which is why the transverse mounting is desired for the MLA analysis. The MLA would raster in a north-south direction (ie up-down when looking at Figure 1) to ensure a true cross section of mineral phases is analyzed. Depending upon the type of material, each mount can display more than 50,000 particles. The Figure 1 inset particle shows textural detail of a pyrite particle with a fracture line (~75um long x ~5 um wide) that contains oxidation product iron hydroxide containing trace copper, lead, zinc and arsenic (listed from largest to smallest content). This detail is available for any particle.

Figure 1. MLA phase-classified particle map: -1190/+600µm size fraction (colour: red = pyrite; blue = copper phases; black = sulphides; green = carbonates; gray = oxides; pink = silicates].

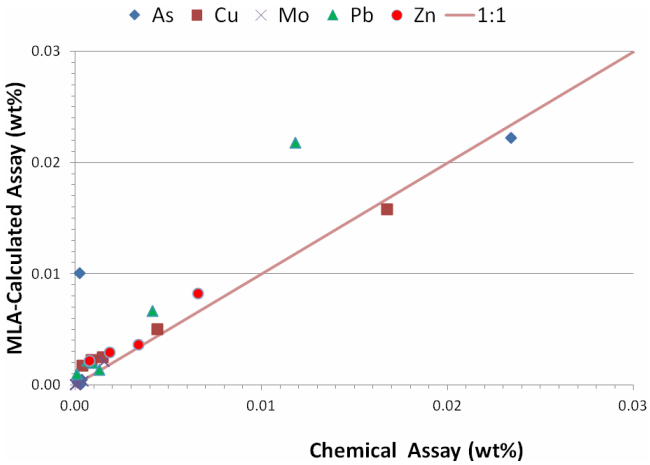

Figure 2. Reconciliation of elemental data: MLA calculated assay vs. chemical assay

To verify that the MLA was successful in the measurement and classification of component minerals the chemical analyses for corresponding sample fractions are compared directly with the MLA calculated assay data (Figure 2). Figure 2 compares EOC results from geochemistry and the MLA. Note the very low concentration scale of the plot showing MLA data can generate quality results.

The MLA data also supplies information about particle and grain size distribution for each mineral phase, particle properties (eg area, perimeter, Hull perimeter, aspect ratio, angularity), mineral association and degree of exposure of a mineral at the particle surface (eg liberated, partially or fully locked). Table 4 shows a typical example of association and degree-of-liberation (ie locking) data. The summed components show the portion of sample particles included in a specific size fraction or mineral group. In Table 4, the "Size Fraction SUM" reflects the total quantity of arsenic-bearing mineral phases measured in each size fraction. Note that 26.8 wt% (13.5+13.3) of arsenic-bearing phases are in sub-105µm particles (represents 72% of total arsenic-bearing phases) and mainly associated with silicates. This suggests silicates must either be reacting with ARD and incorporating arsenic as a new phase or providing a matrix for arsenic-bearing phases to precipitate. Reviewing the particle images revealed that both mechanisms were occurring.

Table 4. MLA arsenic mineral association and locking: before and after diagnostic sequential leach

Sample	Before Leach (wt%)						After Leach (wt%)				
Mineral / µm	-1190/+600	-600/+297	-297/+105	-105/+53	-53	Calculated SUM	-1190/+600	-297/+105	-105/+53	-53	Calculated SUM
Liberated	**<0.1**	**0.9**	**0.2**	**5.9**	**11.4**	**18.6**	**0.6**	**4.8**	**1.0**	**13.1**	**19.5**
Sulphide (binary)	<0.1	1.7	<0.1	1.5	0.1	3.3	0.1	0.3	<0.1	1.0	1.4
Carbonate (binary)	1.7	0.4	<0.1	1.2	0.9	4.2	0.2	<0.1	<0.1	0	0.2
Silicate (binary)	1.9	0.5	0.9	2.4	0.4	6.1	0.4	0.8	0.1	0.5	1.7
Other (binary)	<0.1	<0.1	<0.1	0.1	<0.1	0.2	<0.1	<0.1	<0.1	0.1	0.1
Ternary+ (any phase)	0.7	0.7	0.2	2.4	0.5	4.5	0.2	<0.1	<0.1	0.3	0.6
Size Fraction SUM	4.4	4.1	1.5	13.5	13.3	36.8	1.5	5.9	1.2	15.0	23.5

The "Calculated SUM" reflects the nature of all arsenic-bearing mineral phases within the size fractions with respect to liberation. In this sample, 63.2 wt% (100-36.8) of all particles contained no arsenic. "Liberated" minerals are defined as grains that are not associated with other particles (ie "free"). Note that18.6 wt% of arsenic-bearing phases are fully liberated with the majority being of -53µm particle size. The next four lines (ie "Sulphide", "Carbonate", etc) refer to binary associations between arsenic-bearing minerals and one other phase. The "Sulphide", "Carbonate", and "Silicate" have been taken as collective groups, with "Other" reflecting the balance of all other mineral phases. Finally, "Ternary+" refers to the association of three or more mineral phases with at least one arsenic-bearing phase. After the leach there are more liberated arsenic-bearing phases (19.5 wt%). Note that 13.3 wt% (36.8-23.5) of the arsenic-bearing phases have been removed from the sample - coincidently the same quantity that was present in the -53µm size fraction before the leach; meanwhile the -105/+53µm material was depleted of As-bearing phases, suggesting smaller particles were more reactive. This information builds on the understanding of weathering processes, specifically phase associations, particle size and phase synergies. In consideration of the smaller particles in Table 4, it could be suggested that the generation and neutralization of acid in waste rock piles (and tailings and exposed rock) is dependent on surface area, not mass.

Once the modal mineralogy, EOC particle and grain size, the EOC MOI associations and their degree of exposure have been determined, the MLA software also makes it an easy matter to physically move the SEM sample stage exactly to the MOI particle for further examination. Using the MLA numerical and image data as a base, particles can be highlighted and driven to using MLA coordinates on the sample mount, and then examined more closely using the SEM and EDS to better understand possible phase synergies (Figure 3).

The SEM photomicrographs in Figure 3 show mineralogical features that are the result of weathering. Figure 3a shows galena (PbS) first altered to lead molybdate in the presence of calcium oxide, then further altered to powellite ($CaMoO_4$) and lead oxide in the presence of calcium sulphate and silicate kaolinite

[Conlan *et al.* (in press)]. In the samples of this study, kaolinite-smectite phases were often seen associated with an outer precipitate layer on molybdenite (MoS_2) which perhaps indicates its ability to attenuate molybdenum and/or lead. Figure 3b shows a rare example of galena locked by a rim of powellite-calcium oxide. In this study wulfenite ($PbMoO_4$) was often seen in the presence of molybdenite and lead cations. This particle suggests that galena was locked in calcite and the alteration began from the particle exterior. Figure 3c shows molybdenite locked between rhodochrosite ($MnCO_3$) and a calcium sulphate-oxide phase (trace manganese, copper, zinc). Noting no alteration of the molybdenite, even though it is in the presence of calcium, may indicate that manganese (Mn) retards molybdenite dissolution. Figure 3d shows that the galena host particle developed cracks in which lead oxide was generated. The lead oxide flowed into fractures in the surrounding phases and precipitated. In the presence of calcite (which may underlie the entire particle) wulfenite was formed as molybdenum-containing cations in the aqueous NRD drainage contacted the sites. This could indicate that calcium ions and lead oxide in a basic environment lead to lead molybdate formation. It should be noted that each EOC MOI in Figure 3 is less than 40 µm in size and would require a significant amount of manual labour to locate if MLA technology was not used. With the use of the MLA the EOC particles, as well as a minimum of 20,000 others, were analyzed within one hour. By using the MLA for these scoping studies, the mineralogical data has exposed suggestion of silicate buffering or EOC attenuation, sites of sulphide armouring, and potential weathering mechanisms.

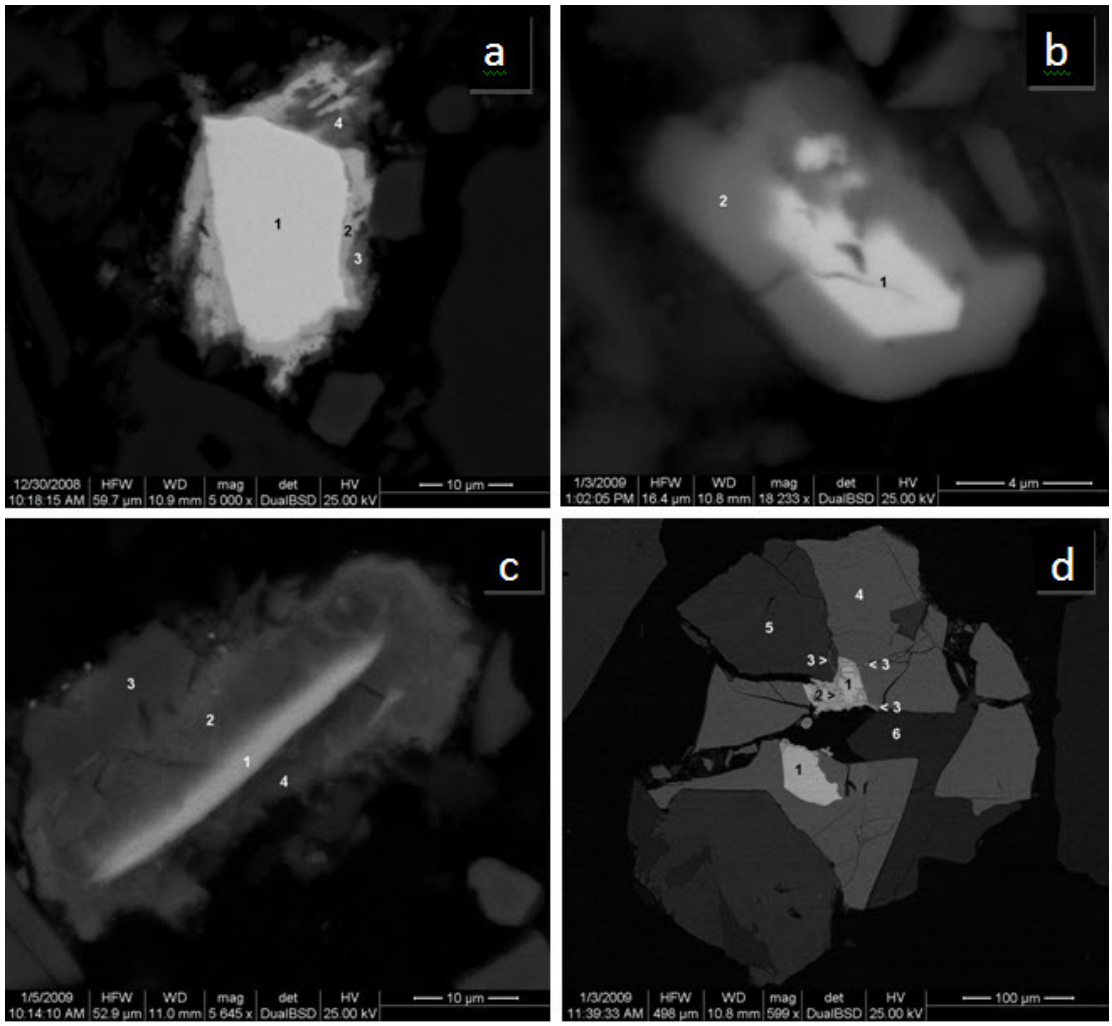

Figure 3. SEM images: (a) Endoskarn waste rock – galena (1) with inner rim of wulfenite and Ca Oxide (2) and outer rim of powellite-gypsum-lead oxide-kaolinite (3, 4); (b) Marginal Cu waste rock – galena (1) with rim of powellite and calcium oxide (2); (c) Endoskarn waste rock – molybdenite (1) locked between

rhodochrosite (2) and gypsum-manganese (Cu, Zn) oxide (4), with calcite (3); (d) Marginal Cu waste rock – complex particle of galena (1), lead oxide (2), chalcopyrite (4), calcite (6), wulfenite-lead oxide (3) and epidote (5).

Through the use of the MLA it can be clearly demonstrated that alteration of sulphides and the sequestering of EOC is a progressive process producing complex mineralogical changes and a variety of intermediate phases dominating different stages of weathering. If the particles of this study were typical of an entire site, it may suggest novel approaches to modeling oxidation weathering. This modeling could affect the selection of mitigation technologies or mine closure requirements.

Future Directions

The visual mineralogical features shown here are supported with quantitative MLA data for particle/grain size and shape, elemental composition, degree of liberation, mineral association, mineral exposure (availability) and perhaps provide an indication of texture. While it is common in mineral processing to study modal mineralogy and mineral liberation, it is less common in geochemical studies.

To strengthen these MLA analyses, their associated assay reconciliation and data interpretation, it is recommended that mineral chemical data be obtained using EPMA (with detection limit 0.01 wt%) and inserted into the MLA X-ray mineral classification standard (detection limit 0.1-0.5 wt%).

The MLA results, in conjunction with other modes of analysis, such as geochemistry and surface analysis such as X-ray photoelectron spectroscopy (XPS), time-of-flight secondary ion mass spectrometry (TOF-SIMS), and X-ray absorption near-edge structure (XANES) will improve our understanding of waste rock weathering processes.

To further improve on the specific MLA results the superior energy stability and intensity of the field emission gun (FEG) SEM could be used. It is equipped with a small probe size (ie 10 times smaller than a regular SEM tungsten filament) for better imaging resolution and delivers decreased data acquisition time (up to 30% faster sample throughput).

Conclusions

- MLA technology can deliver useful and comprehensive mineralogical data which can be applied to metallurgical processing and environmental assessment.
- The MLA is a quantitative mineralogy technique that can be used to rapidly identify mineralogy, mineral association, and liberation (eg locating and studying EOC MOI in rims/fractures or surface-adsorbed precipitate of host particles). The MLA technology can quickly locate individual mineral phases both virtually (ie in stored computer memory) and physically (ie on the sample mount surface). MLA analysis can be as detailed as the operator desires. An MLA analysis of 20,000 particles for basic analysis can be obtained in as little as an hour with spatial resolution of 0.1 µm.
- The mineralogical features determined using the MLA can be used to improve understanding of environmental impact and enable more accurate prediction for designing mine closure. This would greatly improve planning and cost estimates.
- The MLA can be used in conjunction with other technologies (eg transmission electron microscopy (TEM), TOF-SIMS, XANES, XPS, atomic force microscopy (AFM), EPMA, computed tomography (CT)) to determine weathering mechanisms.
- The MLA can be used to diagnose plant circuits, tailings drainage, heap leach behaviour and waste rock drainage. In terms of application, the value of finding trace occurrences of rare secondary alteration phases can be equated to finding valuable metal-bearing phases lost to the tailings.

Acknowledgements

The researchers thank Teck Resources Limited, Natural Sciences and Engineering Research Council of Canada, and Compañía Minera Antamina, S.A. for the funding to make this project possible. The researchers would like to thank Compañia Minera Antamina for supplying the samples and encouraging the study. The researchers would like to thank Teck Metals Ltd. for permission to publish this paper. Appreciation is extended to Teck Metals Ltd. technologists in preparing the samples. Editorial assistance is appreciated from co-authors and Teck's Nichola McKay and Fran Noone. This work was performed as part of a joint project between Compañia Minera Antamina, University of British Columbia and Teck Resources Limited.

References

Alpers, C. N., Blowes, D. W., Nordstrom, D. K., Jambor, J. L. (1994) Secondary minerals and acid-mine water chemistry. In Short Course Handbook on Environmental Geochemistry of Sulfide Mine Wastes, Waterloo, Ontario, May 1994. Mineralogical Association of Canada. p. 247-270.

Álvarez-Valero, A. Pérez-López, R., Matos, J., Capitán, M., Nieto, J., Sáez, R., Delgado, J., Caraballo, M. (2008) Potential environmental impact at São Domingos mining district (Iberian Pyrite Belt, SW Iberian Peninsula): evidence from a chemical and mineralogical characterization. Environmental Geology, Vol. 55(8), pp 1797-1809.

Atkinson, W.W.Jr., Erickson, A.J.Jr. (1984) Concepts in core logging and mapping of mineral deposits: a practical example. In: A.J. Erickson Jr. (Ed), Applied Mining Geology, pp 1-8, Littleton, CO: Society for Mining, Metallurgy, and Exploration.

Chandra, A.P., Gerson, A.R. (2009) A review of the fundamental studies of the copper activation mechanisms of selective flotation of the sulphide minerals, sphalerite and pyrite. Advances in Colloid and Interface Science, Vol. 145, pp 97-110.

Conlan, M.J.W., Mayer, K.U., Blaskovich, R.J., Beckie, R.D. (in press) Solubility controls for molybdenum in neutral rock drainage. Geochemistry: Exploration, Environment, Analysis Decision.

Drever, J.I. (1988) The geochemistry of natural waters. Prentice Hall, Englewood Cliffs, New Jersey, 437 p.

Druschel, G.K., Baker, B.J., Gihring, T.M., Banfield, J.F. (2004) Acid mine drainage biogeochemistry at Iron Mountain, California. Geochemical Transactions, Vol. 5(2), pp 13-32.

Fandrich, R., Gu, Y., Burrows, D., Moeller, K. (2007) Modern SEM-based mineral liberation analysis. International Journal of Mineral Processing, Vol. 84(1-4), pp 310-320.

Gotlieb, P., Wilkie, G., Sutherland, D., Ho Tun, E. (2000) Using quantitative electron microscopy for process mineralogy applications. Journal of Minerals and Materials Characterization and Engineering, Vol. 52(4), pp 24-27.

Gu, Y. (2003) Automated scanning electron microscope based mineral liberation analysis: an introduction to JKMRC/FEI Mineral Liberation Analyzer. Journal of Minerals and Materials Characterization and Engineering, Vol. 2(1), pp 33-41.

Lorenzen, L. (1995) Some guidelines to the design of a diagnostic leaching experiment. Minerals Engineering, Vol. 8(3), pp 247-256.

Lotter, N.O., Kowal, D.L., Tuzun, M.A., Whittaker, P.J., Kormos, L.J. (2003) Sampling and flotation testing of Sudbury Basin drill core for process mineralogy modelling. Minerals Engineering, Vol. 16, pp 857-864.

McKay, N., Wilson, S., Lacouture, B. (2007) Ore characterization of the Aqqaluk deposit at Red Dog. In: 39th Annual Meeting of the Canadian Mineral Processors, Ottawa, Paper #5, January 23-25, pp 55-74.

Petruk, W. (2000) Applied mineralogy in the mining industry. Amsterdam; New York, Elsevier Science BV, 268pp.

Wang, H., Bigham, J., Tuovinen, O. (2007) Oxidation of marcasite and pyrite by oxidizing bacteria and archaea, Hydrometallurgy, Vol. 88(1-4), pp 127-131.

Appendix – MLA Mineral Groupings Based on EOC*

*element(s) in parentheses is part of phase make-up, though trace, as determined by EDS analysis

Antimony, Sb
Bismutostibiconite, Stibnite, Watanabeite(Zn)

Arsenic, As
Arsenopyrite, Enargite, Enargite(Zn), FeOxyHydroxide(CuPbZnAs), FeSulphate(CuAsMoZn), Fornacite(Ca), RealgarOrpiment, Siderite(AsMnZnCu), Tennantite(Zn), Tyrolite(Pb), Watanabeite(Zn), Molybdofornacite(Zn)

Copper, Cu
Apatite(CuPbZn), Bornite, Chalcocite, Chalcopyrite, Chalcopyrite(Pb), Chalcopyrite(Zn), Cuprite, Enargite, Enargite(Zn), FeCuSilicate, FeOxyhydroxide(CuPbZnAs), FeSulphate(CuAsMoZn), Fornacite(Ca), Grunerite(PbCuZn), Jarosite(Cu), Linnaeite(NiCuZn), Malachite, MicaAltered(CuZn), (MoCaSi)Oxide, (MoCa)Sulphate, Molybdofornacite(Zn), MoSilicate, Otavite(ZnCu), Paratacamite, (PbMo)Oxide, Powellite, Pyrite(Cu), Siderite(AsMnZnCu), Sieginite(CuFe), Smithsonite, Sphalerite(Cu), Tennantite(Zn), TitaniteMix(PbCu), TrampMetal, Tyrolite(Pb), Watanabeite(Zn), Wulfenite

Lead, Pb
Apatite(CuPbZn), Chalcopyrite(Pb), FeOxyhydroxide(CuPbZnAs), Fornacite(Ca), Galena(Se), Galenobismutite, Grunerite(PbCuZn), Molybdofornacite(Zn), (MoSi)Oxide, (MoCaSi)Oxide, (PbMo)Oxide, PbOxide(Zn), Powellite, TitaniteMix(PbCu), Tyrolite(Pb), Wulfenite

Molybdenum, Mo
FeSulphate(CuAsMoZn), (MoSi)Oxide, (MoCaSi)Oxide, (MoCa)Sulphate, Molybdenite, Molybdofornacite(Zn), MoSilicate, (PbMo)Oxide, PbOxide(Zn), Powellite, Wulfenite

Zinc, Zn
AgSulphosalt, Apatite(CuPbZn), Chalcopyrite(Zn), Enargite(Zn), FeOxyhydroxide(CuPbZnAs), FeSulphate(CuAsMoZn), Goslarite, Grunerite(PbCuZn), Linnaeite(NiCuZn), MicaAltered(CuZn), (MoCa)Sulphate, Molybdofornacite(Zn), Otavite(ZnCu), Paratacamite, PbOxide(Zn), Powellite, Siderite(AsMnZnCu), Smithsonite, Sphalerite, Sphalerite(Cu), Tennantite(Zn), TrampMetal, Tyrolite(Pb), Watanabeite(Zn), Willemite, Wulfenite, Wulfingite

Acronyms

AAS	Atomic Absorption Spectrophotometry
AFM	Atomic Force Microscopy
BSE	Back Scatter Electron
CT	Computed Tomography
EDS	Energy Dispersive Spectrometer
EOC	Element Of Concern
EPMA	Electron Probe Microanalysis
FEG	Field Emission Gun
(G)XMAP	Grain X-ray Map
ICP	Inductively Coupled (Argon) Plasma
MLA	Mineral Liberation Analyzer
MOI	Mineral Of Interest
NRD	Neutral Rock Drainage
QEMScan	Quantitative Evaluation of Minerals by Scanning electron microscopy
SEM	Scanning Electron Microscope
SPL (XBSE, XMAP, DZ, X)	Sparse Phase Liberation (Extended BSE, X-ray Map, Dual Zoom, X-ray)
TEM	Transmission Electron Microscopy
TOF-SIMS	Time Of Flight-Secondary Ion Mass Spectrometry
XANES	X-ray Absorption Near-Edge Structure
XPS	X-ray Photoelectron Spectroscopy
XRD	X-Ray Diffractometer